ISSN 2457 – 5275 (Online, English)
ISSN 1842 – 4074 (Print, Online, Romanian)

March 2020
Volume 26
Number 1
4 th Series

RoJAE

Romanian Journal of Automotive Engineering

SIAR
The Journal of the Society of Automotive Engineers of Romania
www.siar.ro
www.ro-jae.ro

RoJAE
Romanian Journal of Automotive Engineering

Societatea Inginerilor de Automobile din România
Society of Automotive Engineers of Romania
www.siar.ro

SIAR – The Society of Automotive Engineers of Romania is the professional organization of automotive engineers, an independent legal entity, non-profit, active member of FISITA (Fédération Internationale des Sociétés d'Ingénieurs des Techniques de l'Automobile - International Federation of Automotive Engineering Societies) and EAEC (European Cooperation Automotive Engineers).

Founded in January 1990 as a professional association, non-governmental, SIAR's main objectives are: development and increase the exchange of professional information, promoting Romanian scientific research results, new technologies specific to automotive industry, international cooperation.

Shortly after its constitution, SIAR was affiliated to FISITA - International Federation of Automotive Engineers and EAEC - European Conference of Automotive Engineers, thus ensuring full involvement in specific activities undertaken globally.

In order to help promoting the science and technology in the automotive industry, SIAR is issuing 4 times a year rIA - Journal of Automotive Engineers (on paper in Romanian and electronically in Romanian and English).

The organization of national and international scientific meetings with a large participation of experts from universities and research institutes and economic environment is an important part of SIAR's. In this direction, SIAR holds an annual scientific event with a wide international participation. The SIAR annual congress is hosted successively by large universities that have ongoing programs of study in automotive engineering.

Developing relationships with the economic environment is a constant concern. The presence in Romania of OEMs and their suppliers enables continuous communication between industry and academia.

A constant priority in SIAR's activity is to ensure optimal framework for collaboration between universities and research, industry and business specialists.

SIAR – Society of Automotive Engineers of Romania is member of:

FISITA - International Federation of Automotive Engineers Societies
www.fisita.com
EAEC - European Automotive Engineers Cooperation

RoJAE
Romanian
Journal of Automotive Engineering

CONTENTS

Volume 26, Issue No. 1 **March 2020**

The RoJAE's articles are included in the *„Ingineria automobilului"* magazine (*ISSN 1842 – 4074*), published by SIAR in Romanian.

The articles published in *„Ingineria automobilului"* magazine are indexed by Web of Science in the *„Emerging Source Citation Index (ESCI)"* Section.

Web of Science

Clarivate Analytics

RoJAE 26(1) 1 – 30 (2020)

ISSN 2457 – 5275 (Online, English)
ISSN 1842 – 4074 (Print, Online, Romanian)

The journals of SIAR are available at the website ***www.ro-jae.ro.***

RoJAE
Romanian
Journal of Automotive Engineering

The Journal of the Society of Automotive Engineers of Romania
www.ro-jae.ro
www.siar.ro

Production office:
The Society of Automotive Engineers of Romania (Societatea Inginerilor de Automobile din România)
Facultatea de Transporturi, Splaiul Independentei Nr. 313
060042 Bucharest ROMANIA Tel.: +4.021.316.96.08 Fax: +4.021.316.96.08 E-mail: siar@siar.ro
Staff: Professor Minu MITREA, General Secretary of SIAR

Subscriptions: Published quarterly. Individual subscription should be ordered to the Production office. Annual subscription rate can be found at SIAR website ***http://www.siar.ro.***

ISSN 2457 – 5275 (Online, English)
ISSN 1842 – 4074 (Print, Online, Romanian)

THE PNEUMATIC PROPULSION SYSTEM OF A ROAD VEHICLE

Catalin CHIOREANU, Tudor MITRAN*, Sorin PATER, Marius PELE

University of Oradea, Str. Universitatii, Nr. 1, 410087 ORADEA, Romania

(Received 15 September 2019; Revised 05 October 2019; Accepted 02 November 2019)

Abstract: *The paper presents the functional scheme of a pneumatic propulsion system for road vehicles. This includes a high-pressure air tank, a low-pressure air tank and a pneumatic motor that converts the energy stored in the compressed air tank into mechanical work. The design of the pneumatic motor is an innovative one (the authors have no information about such system that has been designed or manufactured worldwide). It takes over the functions of the gear box: the adjustment of the torque and the change of the rotational sense. In order to estimate the autonomy of such a vehicle, one has developed an energy balance of the propulsion system. Based on the energy consumed for the generation of the high pressure compressed air it aims to estimate by calculus the distance that the vehicle can travel. This solution aims to offer a less polluting propulsion systems for the road vehicles. As known, the manufacturing and the recycling technologies for the electric batteries produce polluting materials and emissions.*

Key-Words: *Compressed air. Energy balance. Pneumatic motor. Pneumatic propulsion.*

NOMENCLATURE

α : the cam's rotational angle, rad
ict : the number of cylinders for one torque step, m^2
it : the number of torque steps,
Mcm : the mean torque developed by one cylinder, Nm
n_1 : the maximum rotational speed, rot/min
$\dot{m}_1$: the mass flow that passes from the high-pressure tank to the low-pressure tank, kg/s
$\dot{m}_2$: the mass flow that passes from the low-pressure tank to the pneumatic cylinders, kg/s
V_1 : the volume of the high pressure tank, m^3
R : the air constant, J/(kg.K)
T1 : the temperature of the compressed air inside the high-pressure tank, K
dp/dτ: the variation of the pressure inside the high-pressure tank due to the air consumption in the interval dτ, Pa/s
ρa : the air density, kg/m^3
V_m: the volumetric flow of the air consumed by the pneumatic motor, m^3/s
dr : the driving's wheel diameter, m
nr : the pneumatic motor's maximum rotational speed, rot/min
r0 : is the base circle radius, mm
s(α) : is the function of the piston's displacement, mm

1. INTRODUCTION

The idea of a pneumatic propulsion system is not a novelty. The pneumatic propulsion system for road vehicles should be an alternative to the electric propulsion. The main disadvantages for the electric propulsion are: the fact that the manufacturing and the recycling technologies are pollutant and, at least at this moment, the rechargeable batteries infrastructure involves a great amount of electric current that can lead to failures of the electric grid. Another advantage of this solution is the much shorter time necessary for the compressed air tank to be refilled in comparison to the one necessary for the electric batteries. Some theoretical studies aimed to reveal the strong and the weak points of the pneumatic propulsion systems for road vehicles [1].

* *Corresponding author e-mail:* tudor_mitran06@yahoo.com

ISSN 2457 – 5275 (Online, English)
ISSN 1842 – 4074 (Print, Online, Romanian)

These studies also offer information for the optimal conditions for the operation of such propulsion systems. Other studies in this field were focused on the environmental impact and on the costs of this solution [2]. These studies give information about the feasibility of implementing such propulsion systems and the conditions in this can happen.
The French company Motor Development International (MDI), established in Luxemburg [3] have realized a partnership with Tata Motors [4] in order to develop a large range of road vehicles with a pneumatic propulsion system. All these steps where not been finalized in serial product, although the main construction concepts of the vehicles were enounced.
The most proposed solutions are based on the Internal Combustion Engine cycle, that means that the general construction of the pneumatic motor is similar to the thermal engine. Another possibility is the use of pneumatic cylinders with single or with double action.
The objective of this paper is to present a new, innovative, concept for a pneumatic propulsion system for road vehicles. This is a continuation of the studies presented in a previous paper [5].
The authors have no information about such system that has been designed or manufactured worldwide. It takes over the functions of the gear box: the adjustment of the torque and the change of the rotational sense. The energetic balance should point the performances of the proposed system. Considering the energy conversion, one can estimate efficiencies with close values for both propulsion systems (pneumatic and electric), but the reliability (the safety in operation) and the endurance of the new pneumatic system will be net superior to the ones of the nowadays electric propulsion systems. Based on the theoretical study, one can think about the development of the system and it's practical application.

2. THE FUNCTIONING OF THE PNEUMATIC PROPULSION SYSTEM

In figure 1 is presented the operational scheme of the new proposed pneumatic propulsion system [6].

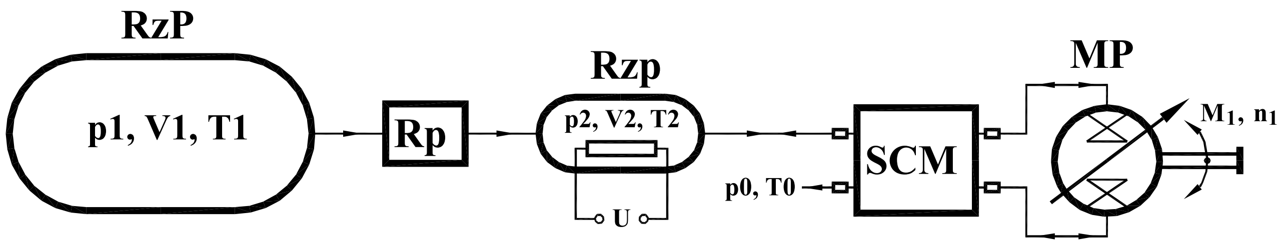

Figure 1. The functioning scheme of the pneumatic propulsion system

The system consists of the following main components: the high-pressure air tank RzP; the pressure regulator Rp; the low-pressure air tank Rzp; and the pneumatic motor with stepped torque adjustment MP. The pneumatic motor takes over and transforms the pneumatic energy from the low-pressure air tank in mechanical energy, generally under the form of a rotational movement, with the following parameters: the motor torque (M_1) and the rotational speed (n_1). These parameters can be adjusted by modifying the motor torque developed by the pneumatic motor. The adjustment of the rotational torque can be done in steps through the motor command system (SCM). Also, through the SCM system one can realize the braking of the vehicle with the recovery of the braking energy (by passing the motor into compressor mode) and, also, the inversion of the vehicle's moving sense.
The propulsion system operates as follow: the pneumatic motor (MP) takes over the pneumatic energy from the low-pressure tank (Rzp) and transforms it into mechanical energy at the parameters necessary for the actuation of the vehicle's running system. The pressure p2 (0,8 – 1 MPa) and the temperature T2 of the air inside the tank Rzp are maintained constant, so that the pressure and the temperature of the exhaust air from the motor should be approximately equal to the environmental pressure and temperature (p0 and T0). The pressure p1 of the air inside the tank RzP varies due to the consumption, from the maximum value p1 = p1max = 20 – 30 MPa, to a minimum value p1 = p1min = p2.
The pneumatic motor with stepped variable torque is a reversible pneumatic machine with stepped adjustment of the rotational torque. It is composed of more identical adjustment steps successively connected to the pneumatic energy source [6].
The functional scheme of the variable stepped adjustment pneumatic motor is presented in figure 2.

ISSN 2457 – 5275 (Online, English)
ISSN 1842 – 4074 (Print, Online, Romanian)

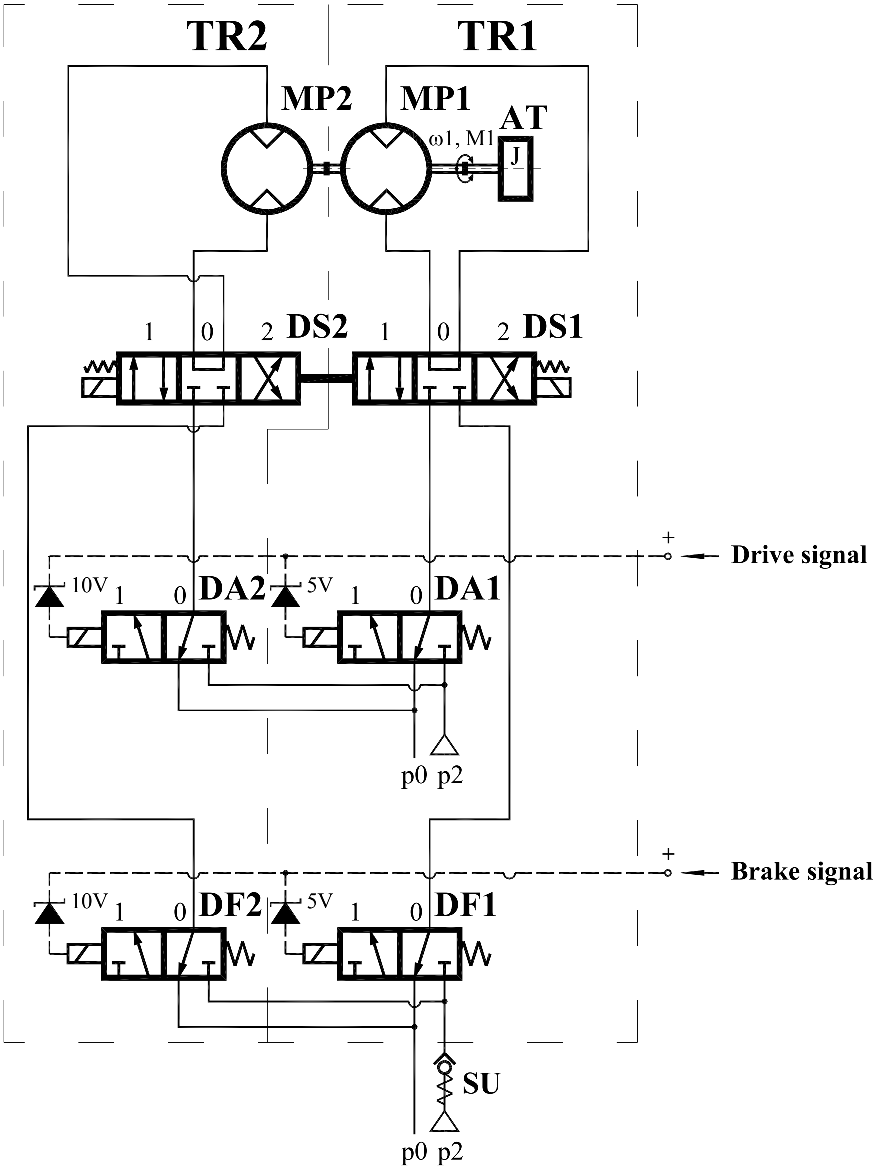

Figure 2. The functional scheme of the variable stepped adjustment pneumatic motor.

In the figure 2 it is presented the functional scheme of the pneumatic motor with two steps of the torque adjustment (TR1 and TR2). The TR1 torque adjustment consists of: the pneumatic motor (MP1) with constant capacity sense distributer DS1, for the change of the rotational sense: actuation distributer DA1, for the supply of the motor with compressed air; braking distributer DF1, for the braking with energy recovery of the braking energy.

The functioning of the pneumatic motor is the following:

1. The start and the acceleration of the rotational movement

Depending on the rotational sense, the sense distributers (DS1) and (DS2) are simultaneously switched on in the position 1 or 2 through an electromagnetic command. The supply of the pneumatic motors of the adjustment steps with compressed air is successively realized by switching the actuation distributers (DA1) and (DA2) in position1, by an electronic system with Zenner diodes. The shaft of the hydraulic motor is moving when the torque M1 developed by the motor is bigger than the resistant torque Mr. The rotational acceleration depends directly proportional on the difference between the rotational torques (M1-Mr) and inversely proportional to the reduced moment of inertia of the powered vehicle.

2. The rotational movement with constant angular speed

The rotational speed is constant when the motor torque is equal with the resistant one (M1=Mr). Depending on the resistant torque variation, the moment developed by the motor is varied in steps through the electronic system with Zenner diodes.

ISSN 2457 – 5275 (Online, English)
ISSN 1842 – 4074 (Print, Online, Romanian)

3. The braking of the rotational movement with the recovery of the braking energy

The pneumatic motors of the adjustment steps turn into a compressor mode. The compressed air produced by the adjustment steps is discharged in the low-pressure tank (Rzp) if at least one of the braking distributers (DF1 or DF2) are in the position 1. For the braking, the actuation distributers are switched in the position 0, and the braking distributers are successively switched in the position 1 through the electronic system with Zenner diodes. The value of the braking torque (Mf) developed by the pneumatic motor depends on the number of the braking activated steps.

3. THE CONSTRUCTIVE SCHEME FOR ONE TORQUE STEP OF THE PNEUMATIC MOTOR

The main parts of the torque step with one pneumatic cylinder are (figure 3): the pneumatic cylinder (CP) with double action and bilateral rod and the cams (Cm1 and Cm2). Under the action of the air pressure, the piston inside the pneumatic cylinder has an alternative rectilinear movement that is transformed, through the cams, into rotational movement. The transmission of the movement from the piston to the cams is done through the sleepers (T1) and (T2). The cams (Cm1) and (Cm2) are fixed on the shafts (A1) and (A2) that are rotating with the same rotational speed, in opposite senses, through a gear transmission or by another way to transmit the rotational movement.

Due to this mode of the cam mechanisms construction, the resultant of the forces F_{21}^{0} (the action force of the element 2 – the tappet, on the element 1 – the cam) that actions on the cams is coaxially to the axis of the piston rods and, in this way, there are no radial forces that should produce friction forces.

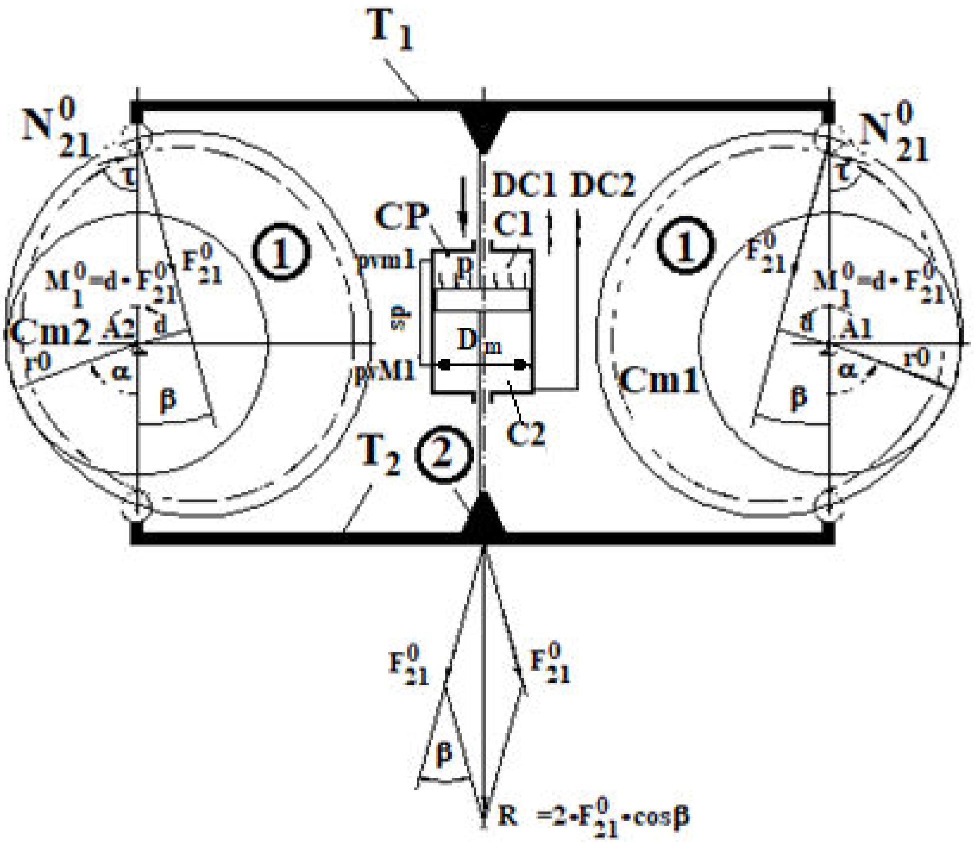

Figure 3. The constructive scheme of the torque step of the pneumatic motor.

The air pressure inside the variable volume chambers C1 and C2 (figure 4) formed inside the pneumatic cylinder is controlled by the distributors (DC1) and (DC2), that alternatively, put in connection the chambers with the low-pressure tank (Rzp). DC1 and DC2 are distributors 3/3 with three connections and three positions. They are switched by the cams CD fixed on a shaft and offset to the Cm1 and Cm2 cams axes with an angle π/2 (fixed on the shaft A2 from the figure 4).

ISSN 2457 – 5275 (Online, English)
ISSN 1842 – 4074 (Print, Online, Romanian)

In the position 0 of the distributor, the chamber inside the pneumatic cylinder is connected to the atmosphere, the exhaust process of the air from the chamber to the atmosphere takes place; in position 1 of the distributor, the chamber inside the pneumatic cylinder is closed and the expansion of the air inside the chamber takes place; in the position 2 of the distributor, the chamber inside the pneumatic cylinder is connected to the low pressure tank Rzp and the chamber is supplied with air under pressure.
When the piston moves from the point pvm1 (the point of minimum volume of the chamber C1) to the point pvM1 (the point of maximum volume of the chamber C1) the motor stroke takes place, and when the piston moves from the point pvM1 to pvm1 the exhaust stroke takes place. When in the chamber C1 takes place the piston's motor stroke, in the chamber C2 takes place the exhaust stroke, and vice versa (figure 4).

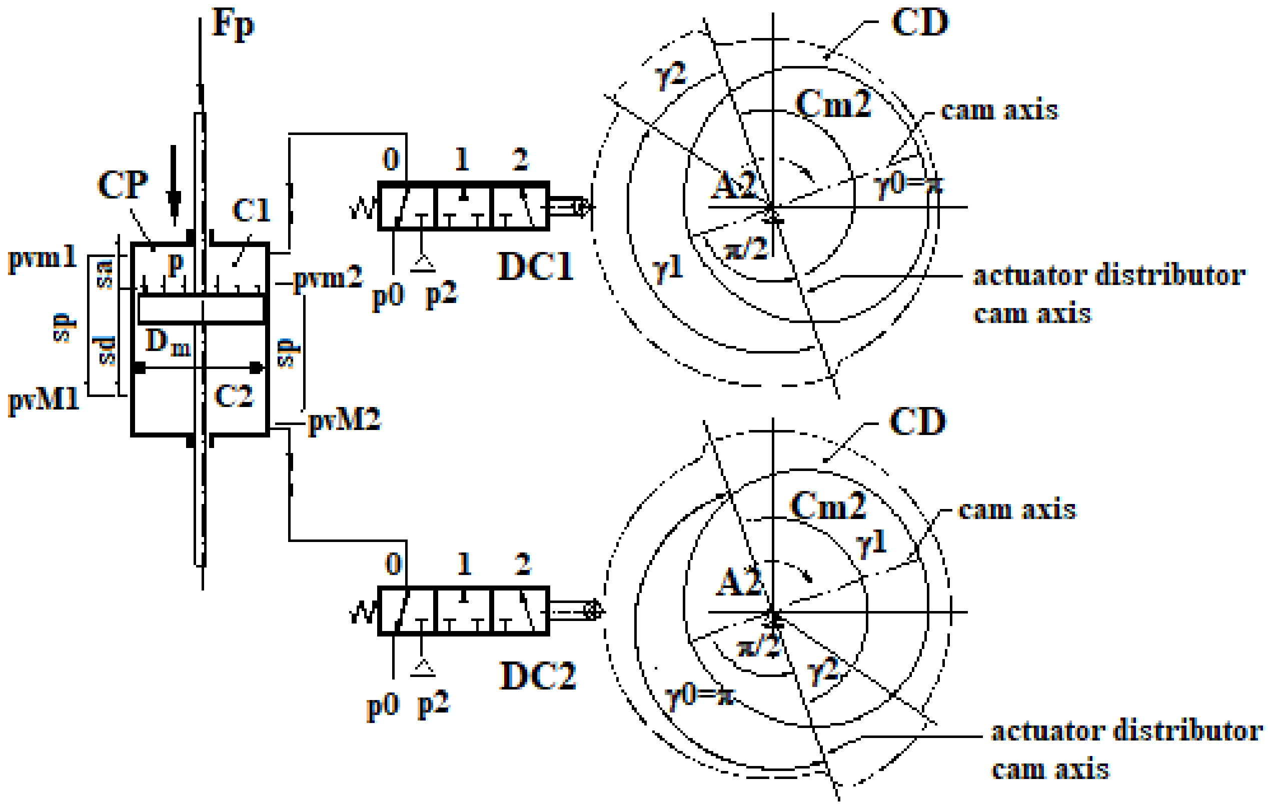

Figure 4. The actuation scheme of the distributers DC1 and DC2.

The piston's motor stroke includes the admission stroke (sa) and the expansion stroke (sd). At the admission stroke, the cam CD switches the distributor in the position 2. During this stroke, the cam CD rotates with the angle γ2. The air parameters inside the cylinder are constant: the pressure pa=p2=ct. and the temperature T2=ct (inside the low-pressure tank). This temperature is maintained constant at the value of the environmental temperature (T0) or the temperature inside the cabin, if the exhaust air is used for air conditioning. This can be done by using a heating system.
At the expansion stroke, the cam CD switches the distributor in the position 1.
During this stroke, the cam CD is rotating with the angle γ1. The air parameters inside the cylinder's chamber are variable: the pressure p=[pa, pd], the temperature T=[Ta, Td]; pa is approximately the pressure inside the low pressure tank; pd is the pressure of the air inside the chamber at the end of the expansion stroke; pd=po+Δpd; p0 is the environmental pressure and Δpd=0,1-0,2 bar is the pressure loss during the exhaust of the air in the atmosphere; by expanding the air near the environmental pressure, one can obtain a maximum efficiency of the pneumatic motor; Ta=T2 where: Ta is the temperature at the beginning of the expansion process.
At the exhaust stroke the cam CD switches the distributor in the position 0. During this stroke, the cam CD is rotating with an angle γ0=π.
The air parameters inside the cylinder's chamber are considered to be constant: the pressure pe=pd and the temperature Te=Td.

ISSN 2457 – 5275 (Online, English)
ISSN 1842 – 4074 (Print, Online, Romanian)

The following notation is used: kp=pa/pd. During the intake process, the volume V of the chamber varies between [0, Va] and in the expansion process the volume varies between [Va, Vt], where: $Va=\pi/4\cdot Dm^2\cdot sa$; $Vt=\pi/4\cdot Dm^2\cdot sp$; Dm is the diameter of the pneumatic cylinder; sa is the intake piston's stroke; sp is the piston's stroke.
One considers that the air expansion is a polytropic process of an exponent n:

$$pa\cdot V_a^n = pd\cdot V_t^n \Rightarrow sa = \frac{1}{k_p^{1/n}}\cdot sp;\ Ta = k_p^{\frac{n-1}{n}}\cdot Td \tag{1}$$

If the pneumatic motor has the cams Cm1 and Cm2 with a sinusoidal profile, the function of the piston's displacement is:

$$s(\alpha) = \begin{cases} \frac{sp}{\pi}\cdot\left[\alpha - \frac{1}{2}\cdot\sin(2\cdot\alpha)\right] & \text{if} \quad \alpha < \pi \\ -\frac{sp}{\pi}\cdot\left(\alpha - \frac{1}{2}\cdot\sin(2\cdot\alpha) - 2\cdot\pi\right) & \text{if } \alpha \geq \pi \end{cases} \tag{2}$$

The rotational angle γ2 of the cam CD that switches at the intake stroke, results from the following equation:

$$sa = \frac{sp}{\pi}\cdot\left[\gamma 2 - \frac{1}{2}\times\sin(2\cdot\gamma 2)\right] \Rightarrow \frac{sp}{\pi}\cdot\left[\gamma 2 - \frac{1}{2}\cdot\sin(2\cdot\gamma 2)\right] - sa = 0 \tag{3}$$

The function for the variation of the air pressure inside the chamber C1 of the cylinder is:

$$pC1(\alpha) = \begin{cases} pa \quad \text{if} \quad \alpha \leq \gamma 2 \\ pa\cdot\left(\frac{sa}{s(\alpha)}\right)^n \quad \text{if} \quad \gamma 2 < \alpha < \pi \\ pd \quad \text{if} \quad \alpha > \pi \end{cases} \tag{4}$$

The function for the variation of the air pressure inside the chamber C2 of the cylinder is:

$$pC2(\alpha) = \begin{cases} pd \quad \text{if} \quad \alpha \leq \pi \\ pa \quad \text{if} \quad \pi < \alpha < \pi + \gamma 2 \\ pa\left(\frac{sa}{sp - s(\alpha)}\right)^n \quad \text{if} \quad \alpha > \pi + \gamma 2 \end{cases} \tag{5}$$

The function for the variation of the pressure angle is:

$$\beta(\alpha) = \operatorname{atan}\left(\frac{1}{r0 + s(\alpha)}\cdot\frac{d}{d\alpha}s(\alpha)\right) \tag{6}$$

The function of the torque developed by the cylinder's chamber C1 is:

$$MC1(\alpha) = \frac{\pi}{4}\cdot Dm^2\cdot\left[r0 + s(\alpha)\right]\cdot\sin\beta(\alpha)\cdot pC1(\alpha) \tag{7}$$

ISSN 2457 – 5275 (Online, English)
ISSN 1842 – 4074 (Print, Online, Romanian)

The function of the torque developed in the chamber C2 of the cylinder is:

$$MC2(\alpha) = \frac{\pi}{4} \cdot Dm^2 \cdot \left[r0 + s(\alpha) \right] \cdot \sin(-\beta(\alpha)) \cdot pC2(\alpha) \tag{8}$$

The function of the total torque developed by one pneumatic cylinder is:

$$M1(\alpha) = MC1(\alpha) + MC2(\alpha) \tag{9}$$

The mean torque developed by one pneumatic cylinder is:

$$MCm = \frac{\int_0^{2\pi} M(\alpha) \cdot d\alpha}{2\pi} \tag{10}$$

In order to reduce the movement's irregularity degree, the engine's torque step can be provided with more cylinders. The cams of one cylinder are fixed on the shafts with an offset regarding the cams from the other cylinders so that the torque irregularity degree should be reduced.
The total torque developed by the pneumatic motor is:

$$M1 = ict \cdot it \cdot MCm \tag{11}$$

The power developed by the engine at the maximum rotational speed is:

$$P = \frac{\pi}{30} \cdot n1 \cdot M1 \left[W \right] \tag{12}$$

In stationary regime, the mass flows are equal:

$$\dot{m}1 = \dot{m}2 \tag{13}$$

$$\frac{dp}{d\tau} \cdot V1 = \frac{dm}{d\tau} \cdot R \cdot T1 \quad \Rightarrow \quad \dot{m}1 = \frac{V1}{R \cdot T1} \cdot \frac{dp}{d\tau} \quad \left[kg/s \right] \tag{14}$$

$$\dot{m}2 = \rho a \cdot \dot{V}m \quad \Rightarrow \quad \dot{m}2 = \frac{p2}{R \cdot T2} \cdot \dot{V}m \quad \left[kg/s \right] \tag{15}$$

The emptying time of the high-pressure tank:

$$\tau g = \frac{V1}{\dot{V}m} \cdot \frac{T2}{T1} \cdot \left(\frac{p1max}{p2} - 1 \right) \tag{16}$$

If all the motor's cylinders have equal dimensions, the air volumetric flow is:

$$\dot{V}m = \frac{\pi}{120} \cdot ict \cdot it \cdot Dm^2 \cdot sa \cdot n1 \tag{17}$$

The maximum distance that the vehicle can travel is:

$$Ad = \frac{\pi}{60} \cdot dr \cdot nr \cdot \frac{V1}{\dot{V}m} \cdot \frac{T2}{T1} \cdot \left(\frac{p1max}{p2} - 1 \right) \tag{18}$$

ISSN 2457 – 5275 (Online, English)
ISSN 1842 – 4074 (Print, Online, Romanian)

If one imposes a certain value of the vehicle's autonomy (the mileage between two refuels), the capacity necessary for the high-pressure tank results from (17).

$$V1=\frac{60}{\pi}\cdot\frac{Ad}{dr}\cdot\frac{\dot{V}m}{nr}\cdot\frac{T1}{T2}\cdot\frac{p2}{p1max-p2} \tag{19}$$

4. NUMERICAL APPLICATION

Based on this algorithm, a numeric application was developed.
The initial data for the calculus is:
- the torque step: the piston's stroke sp=50 mm; the cams rotational speed n1=3000 rot/min; the intake pressure pa=0,8 MPa; the pressure at the end of the expansion pd=0.12 bar; the temperature at the end of the expansion Td=293 K; the exponent of the expansion process n=1.38; the inner diameter of the cylinder Dm=50 mm; the number of the cylinders for one torque step ict=4.
- the pressure inside the low-pressure tank p2=0.8 MPa;
- the maximum pressure inside the high-pressure tank p1max=20 MPa;
- the number of the torque steps i=5;
- the diameter of the driving wheel dr=560 mm;
- the rotational speed of the driving wheel at the maximum rotational speed of the motor nr=1000/min;
- the imposed mileage between two refuels Ad=100 km;

The calculus was developed by using the Mathcad program and it was aimed to determine the capacity of the high-pressure tank needed for a mileage of 100 km between refuels at full load.
The results of this calculus are the following:
- the pressures ratio is: kp=pa/pd=6.67;
- the piston's intake stoke is:

$$sa=\frac{1}{k_p^{1/n}}\cdot sp$$

sa =1/6.679$^{(1/1.38)}$·50 = 12.6 mm;
- the temperature at the beginning of the expansion is:

$$Ta=k_p^{\frac{n-1}{n}}\cdot Td$$

Ta=6.679$^{[(1.38-1)/1.38]}$·293 = 494 K;
- the variation of the pressure inside the chambers of the pneumatic cylinders (Cm1 and Cm2) are presented in the figure 5.

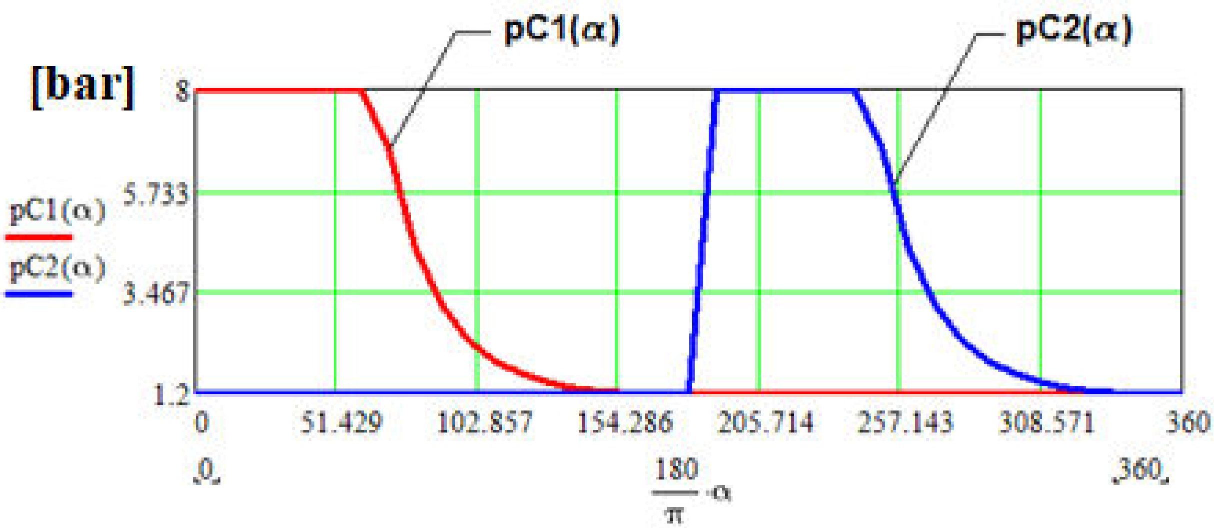

Figure 5. The variation of the pressure inside the cylinder's chambers C1 (pC1) and C2 (pC2)

ISSN 2457 – 5275 (Online, English)
ISSN 1842 – 4074 (Print, Online, Romanian)

- the torques developed in the chambers and the total torque of the pneumatic cylinder are presented in figure 6.
- the mean torque developed by the work of one cylinder is:

$$MCm = \frac{\int_0^{2\pi} M(\alpha)d\alpha}{2\pi} = 9 \ [N \cdot m]$$

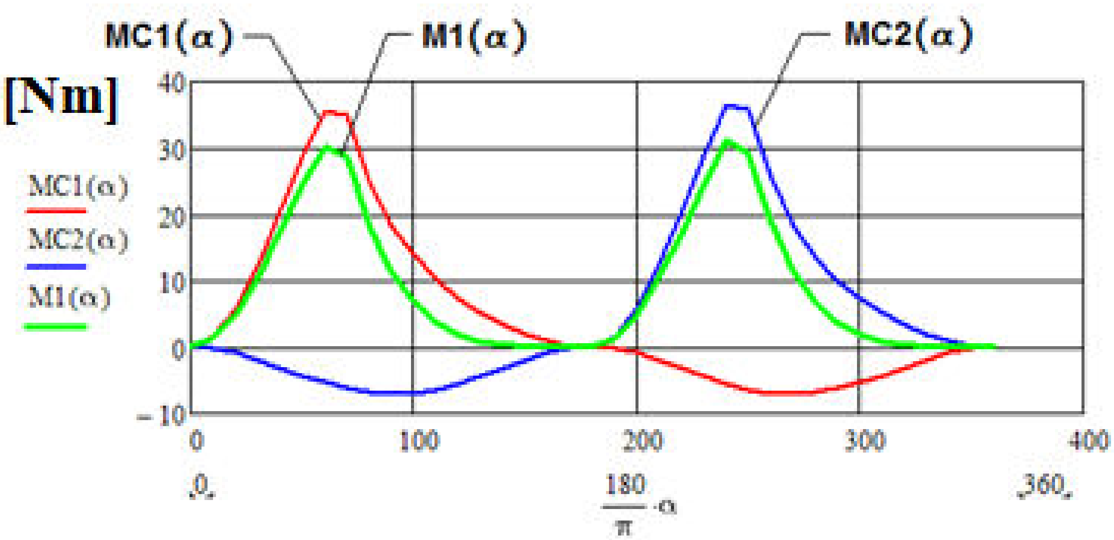

Figure 6. The variation of the torques developed by the of the cylinders C1 (MC1) and C2 (MC2) and of total torque of one step (M1)

- the irregularity degree of one torque step is: δ1=3.449;
- the total torque developed by the pneumatic motor is:

$M1 = ict \cdot it \cdot MCm = 4 \cdot 5 \cdot 9 = 180.2$ N·m

- the power developed by the motor at the maximum rotational speed:

P=π·n1·M1/30=π·3000·180.2/30=56.6 kW;

- the volumetric flow of the air consumed by the motor at the maximum rotational speed is:

$$\dot{V}m = 10^{-9} \cdot \frac{\pi}{120} \cdot ict \cdot it \cdot Dm^2 \cdot sa \cdot n1 = 10^{-9} \cdot \frac{\pi}{120} \cdot 4 \cdot 5 \cdot 50^2 \cdot 12.6 \cdot 3000 = 0.050 \quad m^3/s$$

- the volume of the high-pressure tank for an autonomy of 100 km at full load is:

$$V1 = 10^3 \cdot \frac{60}{\pi} \cdot \frac{Ad}{dr} \cdot \frac{\dot{V}m}{nr} \cdot \frac{T1}{T2} \cdot \frac{p2}{p1max - p2} = 10^3 \cdot \frac{60}{\pi} \cdot \frac{100}{0.7} \cdot \frac{0.05}{1000} \cdot \frac{293}{494} \cdot \frac{8}{200-8} = 3.35 \quad m^3$$

The numerical application is based on deducted relations, that don't take in consideration the losses. The role of the application was to ride the graphics, and the initial values (such as the wheels diameter) have no relevance, because any value is possible in a practical application.
This numerical application is not a designing calculation, it's role is to demonstrate that the obtained values can practically be achieved.
For example, a minibus with the pneumatic motor's power of 56.5 kW, for an autonomy of 100 km., needs a high-pressure tank with a capacity of 3.35 m^3, loaded at maximum pressure of 20 MPa.

5. CONCLUSION

From the previous presented calculation, it results that the pneumatic propulsion is an alternative to the electric propulsion.
The main advantages of the pneumatic propulsion system equipped with the new motor with stepped torque adjustment presented in this paper are the following:
- it realizes all the propulsion functions, with the recovery of the braking energy;
- the dynamics of this propulsion system is superior because the torque developed by one torque step is constant and it does not depend of the rotational speed;

ISSN 2457 – 5275 (Online, English)
ISSN 1842 – 4074 (Print, Online, Romanian)

- one can estimate an efficiency at least equal to the one of the electric propulsion systems. The production of the pneumatic energy for the road vehicle supply is made with high performance electric actioned compressors with an efficiency of 70-80% at values closed to the efficiency of the electric battery recharge. The efficiency of the pneumatic motor is superior to the alternative current motor used for the propulsion of the electric vehicles because those systems need an inverter to convert the DC into an alternative current with variable frequency and voltage.
- the dynamic parameters of the pneumatic propulsion system are not depending on the load degree (the pressure) of the high-pressure tank. They are constant regardless the pressure inside this tank, with the condition that $p1 \geq p2$.

As one can see, the results of the calculus are for an operation at full load.
The range of autonomy in real conditions is higher. Theoretically a road vehicle is functioning at full load for maximum 10% of it's operation.
The results of this study can be extended to different operating regimes, so more accurate results can be taken into consideration for comparing this propulsion system with the electric one.
Also, one must observe that, for the calculus, the pressure of the air inside the high-pressure tank was considered to be p=20 MPa.
The numerical application is based on deducted relations, that don't take in consideration the losses. The role of the application was to ride the graphics, and the initial values (such as the wheels diameter) have no relevance, because any value is possible in a practical application.
This numerical application is not a designing calculation, it's role is to demonstrate that the obtained values can practically be achieved.
For example, a minibus with the pneumatic motor's power of 56.5 kW, for an autonomy of 100 km., needs a high-pressure tank with a capacity of 3.35 m^3, loaded at maximum pressure of 20 MPa.
Recent research [6] show that it is possible to manufacture high pressure air tanks made of carbon fiber. They have a honeycomb structure and can support pressures up to 30 MPa. A great advantage is that, in the case of a crash, the material is brittle and creates no shrapnel.
The tank can be placed on the floor of the vehicle. Also, parts of the car's body can be supplementary high-pressure air tanks.
So, theoretically, an autonomy of 100 km (at full load). can be reached by such a minibus.
This solution is applicable in urban transport for small size vehicles or minibuses.
From an environmental point of view, this solution permits the realization
There are current applications that permit the storage of the compressed air at 40-50 MPa in perfect safety conditions, including the consequences of the car crash [6].

REFERENCES

[1] Bossel, U., *Thermodynamic Analysis of Compressed Air Vehicle Propulsion.* Journal of KONES International Combustion Engines Vol 12, pg. 3-4, 2005
[2] Papson, A., Creutzig, F., Schipper, L., *Compressed Air Vehicles Drive-Cycle Analysis of Vehicle Performance, Environmental Impacts, and Economic Costs.* Journal of the Transportation Research Board, Washington, D.C. No. 2191, pg. 67-7, 2010
[3] *** , MDI Motor Development International, http://www.mdi.lu/produits.php,
[4] Sengupta, D., *Tata Motors to Roll Out Cars That Runs on Compressed Air Instead of Fuels.* The Economic Times March 22, 2008
[5] Mitran, T. Chioreanu, C., Dragomir, G., Fagadar, D., *A propulsion system for urban cars*, AMMA 2018 International Congress of Automotive and Transport Engineering, pp 659-666, Cluj-Napoca, ISBN 978-3-319-94408-1 ISBN 978-3-319-94409-8 (eBook)
[6] ^^^ - Seven Network's Beyond Tomorrow

ISSN 2457 – 5275 (Online, English)
ISSN 1842 – 4074 (Print, Online, Romanian)

CONSIDERATIONS REGARDING THE COMPARATIVE DETERMINATION OF MATERIALS HARDNESS SUBMITTED TO HEAT TREATMENTS

Ramona STOICA*, Daniela VOICU, Laszlo BAROTHI, Radu VILAU

„Ferdinand I" Military Technical Academy, Bdul George Cosbuc, Nr. 39-49, BUCHAREST, Romania

(Received 05 October 2019; Revised 07 November 2019; Accepted 17 December 2019)

Abstract: *Present paper aims to determine a comparative analysis of mechanical part hardness, used in automotive field, by highlighting values measured in different functional surfaces. Therefore, it was used a Fervi D08 hardness tester and it was applied the Rockwell scale in order to enunciate several conclusions regarding the influence of heat treatments on materials, as well as hardness value distribution on the entire surface of a mechanical part. At the same time, it was used a coordinate measuring machine to determine depth of imprinted indentation on tested surfaces. Such an analysis allows evaluating the behaviour of a mechanical part in case of different stresses which occur during functioning.*

Key-Words: *Hardness, Heat treatment, Coordinate measuring.*

1. INTRODUCTION

Hardness testing has the aim to determine physical properties of materials with the purpose to evaluate behavior under the influence of mechanical actions, as well as a quantifiable assertion of results, in order to evaluate whether a metal part meets stress demands that occur during functioning [1].

Main scope of the paper was to determine by measuring the tappet hardness of an internal combustion engine. Tappets (or cam followers) are constituent parts of the distribution system of a motor vehicle, with function to actuate the valves of internal combustion engines [2].

For the experimental tests it was used a mechanical tappet, of cylindrical shape, with a plate at the inferior part which comes in contact with the valves.

The part used for testing was made of alloyed steel and was submitted to tempering (heat treatment) on the entire surface so that it complies with requirements assessed by the operating conditions.

Considering the wearing process of a tappet during functioning, it was performed a comparative analysis of hardness, at the middle point of the cam follower (tappet) and in several points on the exterior circular line of the tappet's plate.

Also, in order to highlight variation of hardness values on the entire longitudinal axis of the tappet, there were performed tests at both ends, in the middle point of the surface (one at the plate end and the other at the tappet's rear, also known as its tail) [2].

There have been processed and analyzed all results obtained from experimental tests, in order to highlight differences regarding mechanical properties determined on multiple surfaces of the same part which was prior submitted to tempering (heat treatment).

2. DEVELOPMENT OF EXPERIMENTAL TESTS

Experimental tests consisted in applying a static method to determine hardness, with the use of a Fervi D018 hardness tester.

The practical part was preceded by a functional checkup of the tester, realized with the use of a reference sample, with inscribed values for Rockwell hardness validation.

Several examples of calibration references are presented in figure 1a).

* *Corresponding author e-mail:* ramona.stoica@mta.ro

ISSN 2457 – 5275 (Online, English)
ISSN 1842 – 4074 (Print, Online, Romanian)

Figure 1.a) Reference sample HRC b) Conical diamond indenter

After verifying the proper functioning of the tester (calibration process) it was selected an appropriate type of indenter based on the analyzed material and taking into account all specifications from specialty literature, as well as the indications provided by the manufacturer of hardness tester [1][3].
Therefore, the tester was equipped with a conical diamond indenter, presented in figure 1b), which is specific to the Rockwell hardness test.
This method is used in case of hardened materials such as tempered alloyed steel (HRC - conical diamond indenter), tools made of hardened alloys (HRA – conical diamond indenter) and soft, malleable or untreated metals (HRB).
In this case, considering the material of the analyzed tappet, it was used the HRC scale [1][3].
The procedure to determine material hardness consisted in [3]:

- cleaning of the tappet’s surface, followed by grinding operation (the abrasion was realized with a grinding machine) so that the analyzed surface is polished, without scratch, rust stains or other defects;
- proper display of the tappet, on a V (Vee) anvil which is used for cylindrical shaped rods or tubing, so that there are eliminated errors specific to testing and reading the imprint made by the indenter. This stage ensures an orthogonal position between the tip of the indenter and the tested surface, but also a fixed position of the tappet under the influence of the indentation force;
- verifying minimal thickness of the tappet so that the material is 10 times higher that the depth of indentation;
- realising the contact between tested surface and indenter, by applying an intial charging force of 10 kgf (10 daN);
- the pressing lever was set to 100 kg (980.7 N);
- pressing the start button of hardness tester, the charging force was automatically loaded so that in the moment of maximum load, the main force was instantly applied. The force is maintained for 5 seconds.
- follow-up, hardness value was read from the tester's screen;
- for result validation there have been performed 5 measurements (one for each middle point at both ends where are the functional surfaces of the tappet and three indentations near the exterior diameter of the tappet's plate).

Testing procedure is depicted in figure 2.

Figure 2. Hardness testing in the middle of tappet's plate

ISSN 2457 – 5275 (Online, English)
ISSN 1842 – 4074 (Print, Online, Romanian)

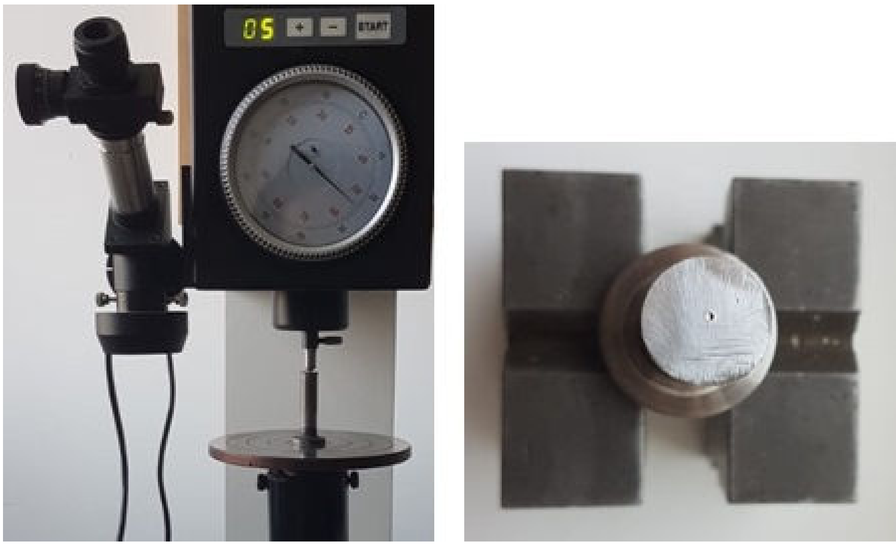

Figure 3. Hardness testing in the middle of tappet's rear (tail)

As it can be observed from figure 2 and figure 3, hardness value in the middle of tappet's plate is 32 HRC. Likewise, the value measured in the middle of tappet's rear was 24 HRC.
Regarding the values obtained from measurements near the exterior diameter of the plate, and considering that the mechanical part reached the end of its life cycle, hardness values obtained in various points on the diameter were different, resulting an average hardness of 38 HRC.

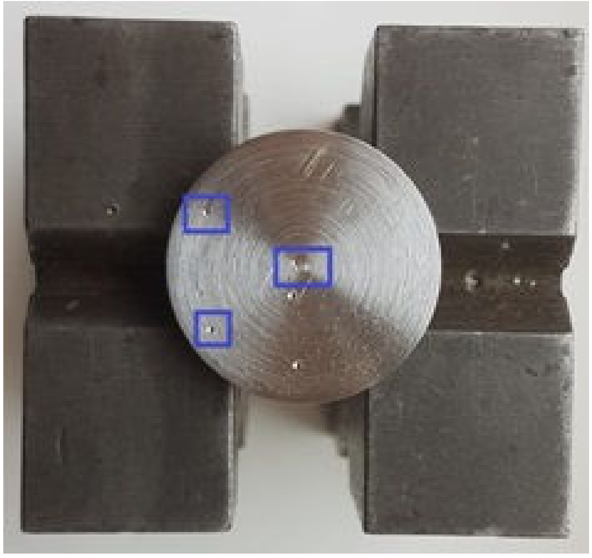

Figure 4. Areas from tappet's plate where hardness was tested

Analysis of results has highlighted that hardness values in superficial layer of tappet is higher than the value measured in the middle of material.
Differences obtained can be attributed to the tempering process, namely:
- holding period for temperature equalization on the entire section of the mechanical part,
- duration of the heating process,
- carbon concentration within the alloy,
- tempering environments, which must be chosen based on the mechanical part diameter and cooling speed etc.

Results obtained with the hardness tester can be validated with the use of a coordinate measuring machine, which allows determining hardness by mathematical computing [1]:

$$HRC=E-e \quad (1)$$

where E is a suitable chosen value, and e is the depth of residual indentation.

ISSN 2457 – 5275 (Online, English)
ISSN 1842 – 4074 (Print, Online, Romanian)

In present paper it was used the coordinate measuring machine, presented in figure 5, for determining the indentation depth in order to compare values obtained on different areas of the tappet.

Figure 5. Coordinate measuring machine

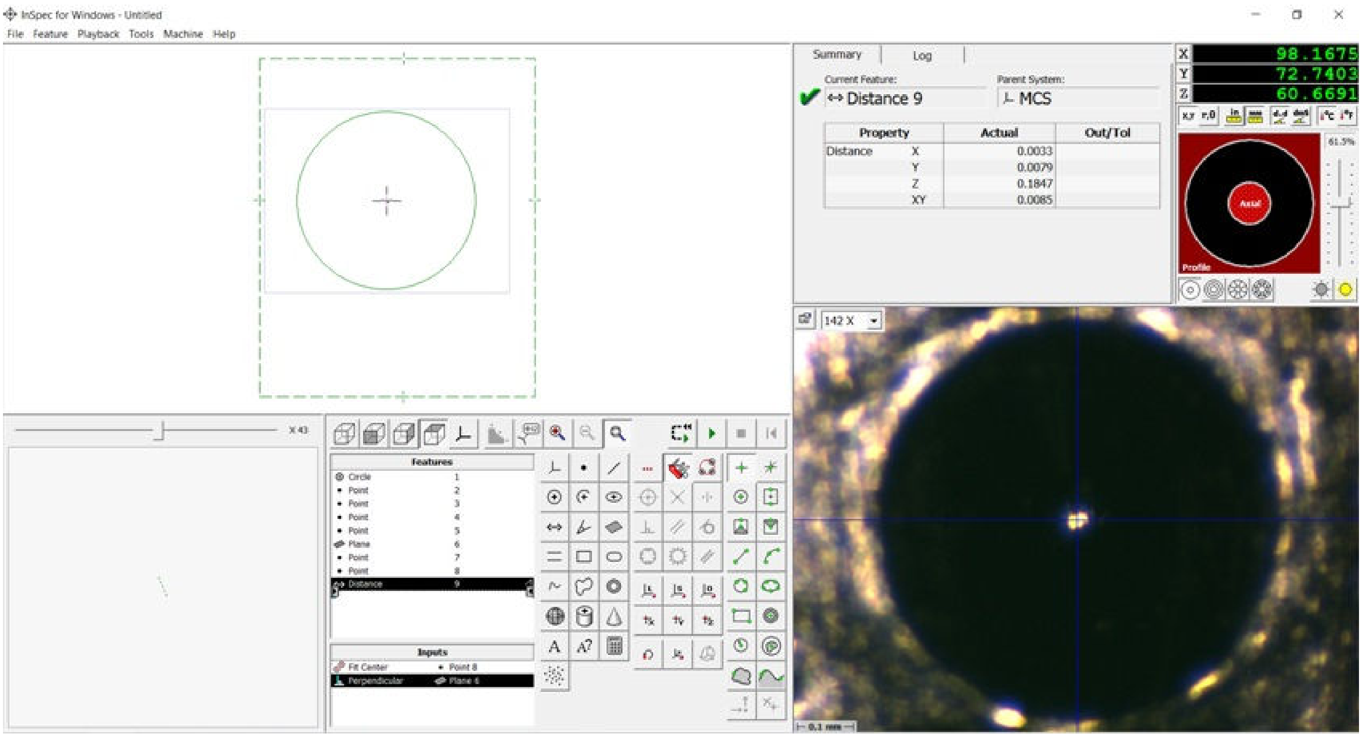

Figure 6. Indentation depth measured in the middle of the tappet's plate

ISSN 2457 – 5275 (Online, English)
ISSN 1842 – 4074 (Print, Online, Romanian)

Several examples of results provided by the coordinate measuring device are presented in figures 6 and figure 7. In the upper-left quadrant of figure 6 is indicated the position of indentation made in material and in the upper-right quadrant are illustrated values of coordinate points of the indentation, as well as the depth of residual mark of 0.184 mm. At the same time, from figure 7, in the upper-left quadrant it can be observed the depth value of each imprint made by the conical diamond indenter, namely 0.139 mm, which is measured on Z axis.

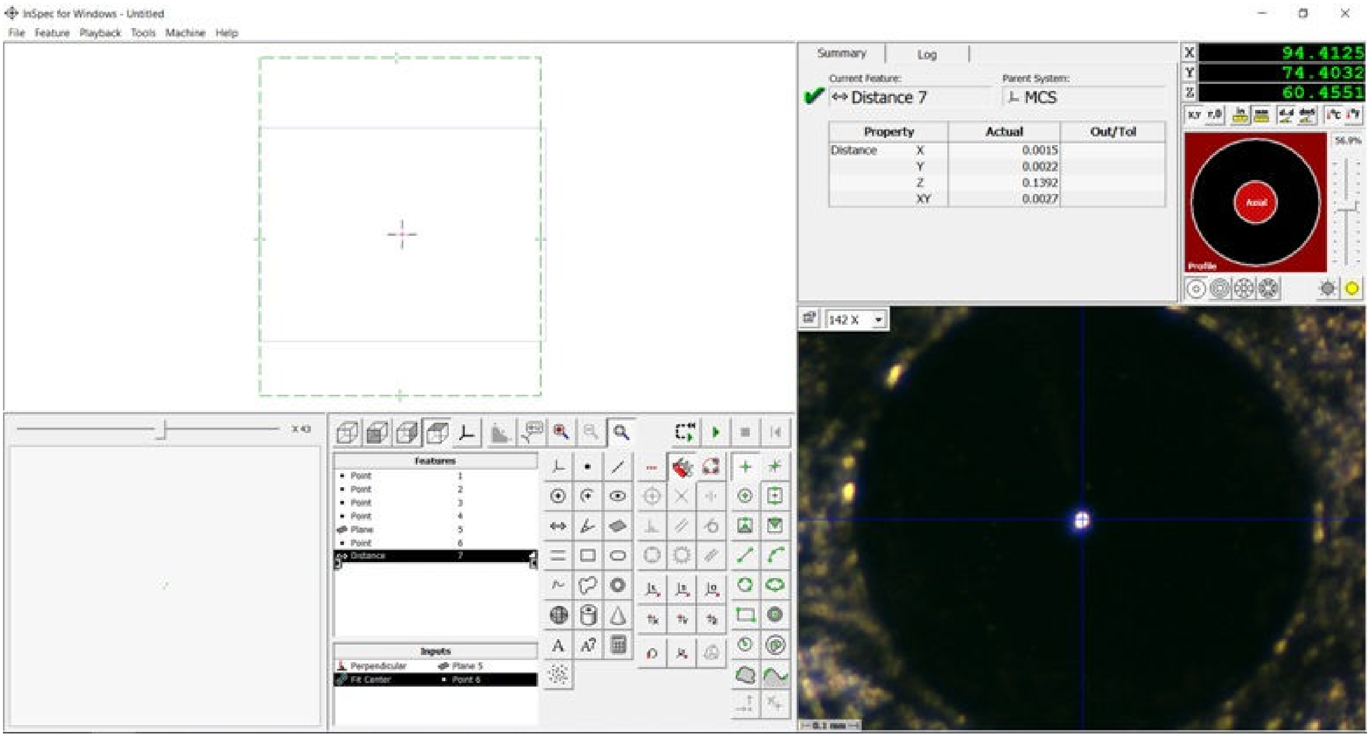

Figure 7. Indentation depth in one point on the exterior diameter of tappet's plate

3. CONCLUSIONS

Present paper had the purpose to list and elaborate phases made for a comparative analysis of mechanical part hardness, in different points on the transverse sectioning plane.
Methodology of experimental research must be applied considering all conventions from specialty literature, as well as the instructions recommended in the hardness tester workbook.
All characteristic stages must be passed through in order to eliminate errors while measuring and reading values.
From the analysis of hardness values, obtained both in the middle of tappet's plate and in several other points near the exterior diameter, it was observed that the heat treatment of tempering which was applied for improved mechanical properties, had different influences on the entire section.
Therefore, in the middle area there have been obtained lower hardness values than on the exterior circular line of the tappet's plate. Possible explanations have been detailed in chapter 2, regarding the procedure of experimental tests.
At the same time, following the analysis of results obtained by using the coordinate measuring machine, it was observed that the imprinted depth of indentation on the surface with 38 HRC hardness was 0.139 mm, whereas the value of indentation depth with 32 HRC hardness value was 0.184 mm, as was to be expected.
Therefore, it is a compulsory request to determine hardness materials in order to certify that a mechanical part can face stress, wearing process etc., depending on its functional usage.

ISSN 2457 – 5275 (Online, English)
ISSN 1842 – 4074 (Print, Online, Romanian)

REFERENCES

[1] Atanasiu, Costică; Canta, Traian; Caracostea, Andrei, *Încercarea materialelor*, vol. I, pag. 130-152, Editura Tehnică, 1989

[2] Frățilă, Gheorghe; Frățilă, Mariana; Samoilă, St., *Automobile. Cunoaștere, întreținere și reparare* Editura didactică și pedagogică, București, 1995, ISBN 973-30-4242-0

[3] *** - Manual de utilizare și întreținere. Durometru pentru banc model D018. Fervi Pro Smart Equipment, 2016

ISSN 2457 – 5275 (Online, English)
ISSN 1842 – 4074 (Print, Online, Romanian)

CYCLIST HEAD TO WINDSHIELD IMPACT ANALYSIS. DEFORMATION AND PERFORATION CASE STUDY

Ovidiu Andrei CONDREA [*], Anghel CHIRU, George TOGĂNEL, Ionuț Alexandru RADU, Rareș Lucian CHIRIAC

Transilvania University of Brașov, Str. Politehnicii Nr. 1, 500024 BRASOV, Romania

(Received 17 October 2019; Revised 21 November 2019; Accepted 05 December 2019)

Abstract: *Some particular types of accidents between motor vehicles and VRU produce partial intrusions of the VRU's body inside the passenger compartment through the vehicle's windshield. Collisions which result in windshield perforations can significantly alter the preconized human-body kinematics, throw distance and injuries, therefore making the reconstruction of the accident more difficult. Due to the complex nature of windshield deformations, the current state-of-art does not allow for the different stages of windshield deformation growth to be simulated in a multibody software. This paper presents a technique for simulating vehicle-VRU impacts with windshield perforations, comprised of locally altering the exterior contour of the vehicle's windshield damaged area, therefore being possible to simulate the intrusion inside the passenger compartment. A vehicle-cyclist crash-test which resulted in a 600 cm^2 windshield perforation and was simulated by applying the presented technique is exemplified as a case study in this paper. The results of the simulations yielded similar dummy kinematics, proving the viability of the presented technique for the kinematic sequence reconstruction of impacts with windshield perforations. An analysis of the influence yielded by the generation of a windscreen perforation over the VRU transport phase and throw distance was also conducted.*

Key-Words: *Cyclist impact, Windshield deformation, Windshield perforation, Multibody simulation.*

NOMENCLATURE

VRU: vulnerable road users

1. INTRODUCTION

Pedestrians and cyclists are regarded as vulnerable road users in traffic due to a high degree of exposure and a significant degree of susceptibility to serious and lethal injuries [3].
In order to improve VRU safety, the kinematic and dynamic behavior of a human body when subjected to an impact with a vehicle must be well comprehended. Accident reconstruction serves as a tool in establishing the causes which lead to an accident and also its effects. The accident reconstruction process is generally extensively conducted through multibody simulations, especially for accidents involving VRU, since the multibody approach offers significantly more data and elements of control than other reconstruction methods such as simplified mathematical models.
The multibody representation which consists of 20 individual articulated bodies is also more consistent in terms of biofidelity than other simplistic approximations.
Accidents between motorized vehicles and VRU are a common concern for forensics and researchers due to the frequently resulting severe or lethal injuries of VRU.
The most severe injuries are generated due to the head-windshield impact, such as skull and facial bone fractures, concussions or diffuse axonal injuries [1]. Depending on the impact configuration, eye injuries can also occur if the face of the VRU impacts the windshield.
Modern laminated windshields have better performances in terms of preventing lacerations and eye injuries compared to the early tempered windshields [2][4], which have been replaced in production for virtually all vehicles. Laminated glass has a composite structure with superior mechanical properties and better energy absorbing capabilities than single glass [10].

[*] *Corresponding author e-mail:* ovidiu.condrea@unitbv.ro

ISSN 2457 – 5275 (Online, English)
ISSN 1842 – 4074 (Print, Online, Romanian)

The PVB interlayer which connects the sheets of laminated glass prevents glass destructuration into multiple large and sharp fragments due to its adhesive properties [10].
Another important safety aspect of the laminated windshields is given by the decreased chances of occupant ejection or VRU intrusion inside the passenger compartment through windshield perforation is prevented, due to their improved penetration resistance [7]. Yet at high impact velocities, depending on the angle between the VRU impacting body zone and the windshield, even laminated windshields may locally fail if the PVB interlayer is ruptured to a certain degree or if delamination occurs.
Delamination is a process which occurs when one or both sheets of windshield glass separate from the PVB interlayer [6]. Generically, windscreen delamination is caused by air entrapment during the fabrication phase or air/moisture admission during the exploitation phase [6].
There is also a natural tendency for laminated windshield failures to result as a windshield ages, since the adhesive properties of the PVB interlayer which connects the two sheets of glass diminish in time due to heat exposure [6]. Therefore, high vehicle impact velocities and windshield delamination can lead to perforations [5] in the windshield structure during impacts with VRU or occupants, as it is the case for older tempered windshields, resulting in intrusions in the passenger compartment.
This particular impact scenario is very difficult to recur in the virtual environment of available multibody software packages since the vehicle is generically represented as a rigid body and the windscreen stages of deformation can’t be simulated.
VRU kinematics are heavily influenced by intrusions in the passenger compartment.
The transport phase which begins after the first contact between the windshield and the head and lasts until the VRU is thrown off the vehicle [8] is significantly longer when windshield perforations are generated in the impact. Consequently, VRU throw distances are also increased and must be distinctively analyzed in relation to impacts without windscreen perforations.
This paper presents a vehicle-cyclist crash-test resulted in windscreen perforation which was simulated in the PC Crash multibody software and describes the used technique which can be applied to simulate any vehicle-VRU impacts with windshield perforations. Using the conditions obtained through the validated simulation and by generating an identical simulation but without perforating the windscreen, a comparative analysis between the cyclist kinematics was conducted in order to assess the influence of windscreen perforations over the transport phase and the resulting throw distance.

2. EXPERIMENTAL TESTING

A vehicle-cyclist crash-test was carried out using an anthropometric dummy, an Opel Corsa B vehicle and a regular bicycle. The dummy was maintained into stationary position with an electromagnetic gibbet support mechanism (shown in Figure 1) and released immediately prior the impact through the means of a laser detection system.

Figure 1. The crash-test scene and the gibbet support mechanism

ISSN 2457 – 5275 (Online, English)
ISSN 1842 – 4074 (Print, Online, Romanian)

The vehicle was braked with a deceleration of 6.5m/s^2 and the vehicle impact velocity was 10.1 m/s.
The bicycle-dummy assembly was hit in the rear extremity by the front of the vehicle at a 00 impact angle. The lateral offset of the collision was 0.25 m.
The crash-test was recorded both with a Fastec HiSpec 5 high speed camera and with a drone.
The dummy was instrumented with a tri-axial accelerometer mounted inside the head's center of gravity in order to record head accelerations, which are shown in Figure 2.

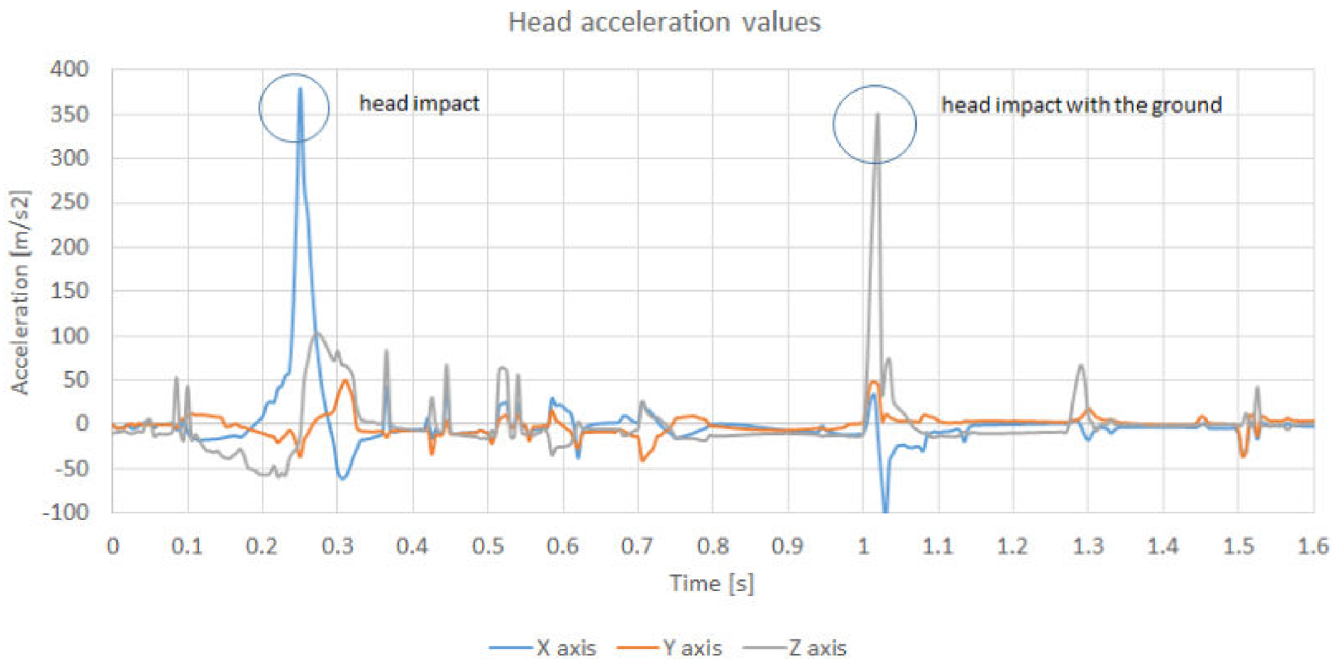

Figure 2. Head acceleration values recorded during the experimental testing

Upon the vehicle-dummy pelvis impact, the head of the dummy impacted the windscreen in the upper right corner, resulting in a perforated windscreen area of nearly 600 cm^2, shown in Figure 3. The length of the deformation measured along the windscreen is 0.45 m, with a corresponding width of 0.2 m.

Figure 3. The windscreen perforation which resulted in the carried-out crash-test

Literature indicates that windscreen perforation is the final stage of windscreen deformation [9]. Initially, a circumferential windscreen deformation is generated upon impact.
As the deformation energy is increased, the circumferential deformed area will record several axes of deformation linked to the center, similar to a spider web.
Upon reaching a threshold value of the deformation energy, the structure of the windscreen in the spider-web deformed area will fail, resulting in a perforation.

ISSN 2457 – 5275 (Online, English)
ISSN 1842 – 4074 (Print, Online, Romanian)

The stages of windscreen deformation are presented in Figure 4.
This aspect was also observed for the carried-out crash-test as the perforated surface of the windscreen holds a distinctive spider-web type of deformation (shown in Figure 5), which is approximately concentric to the perimeter of the perforated surface.

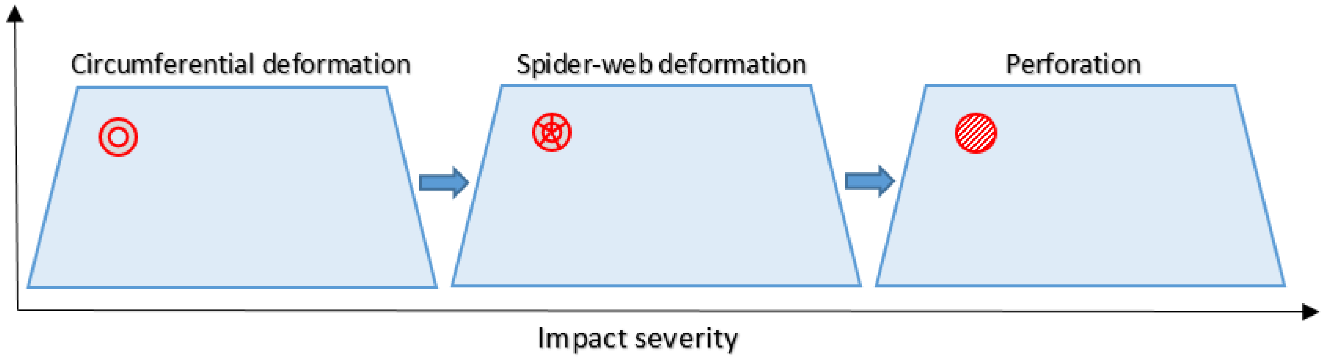

Figure 4. The stages of windscreen deformation [9]

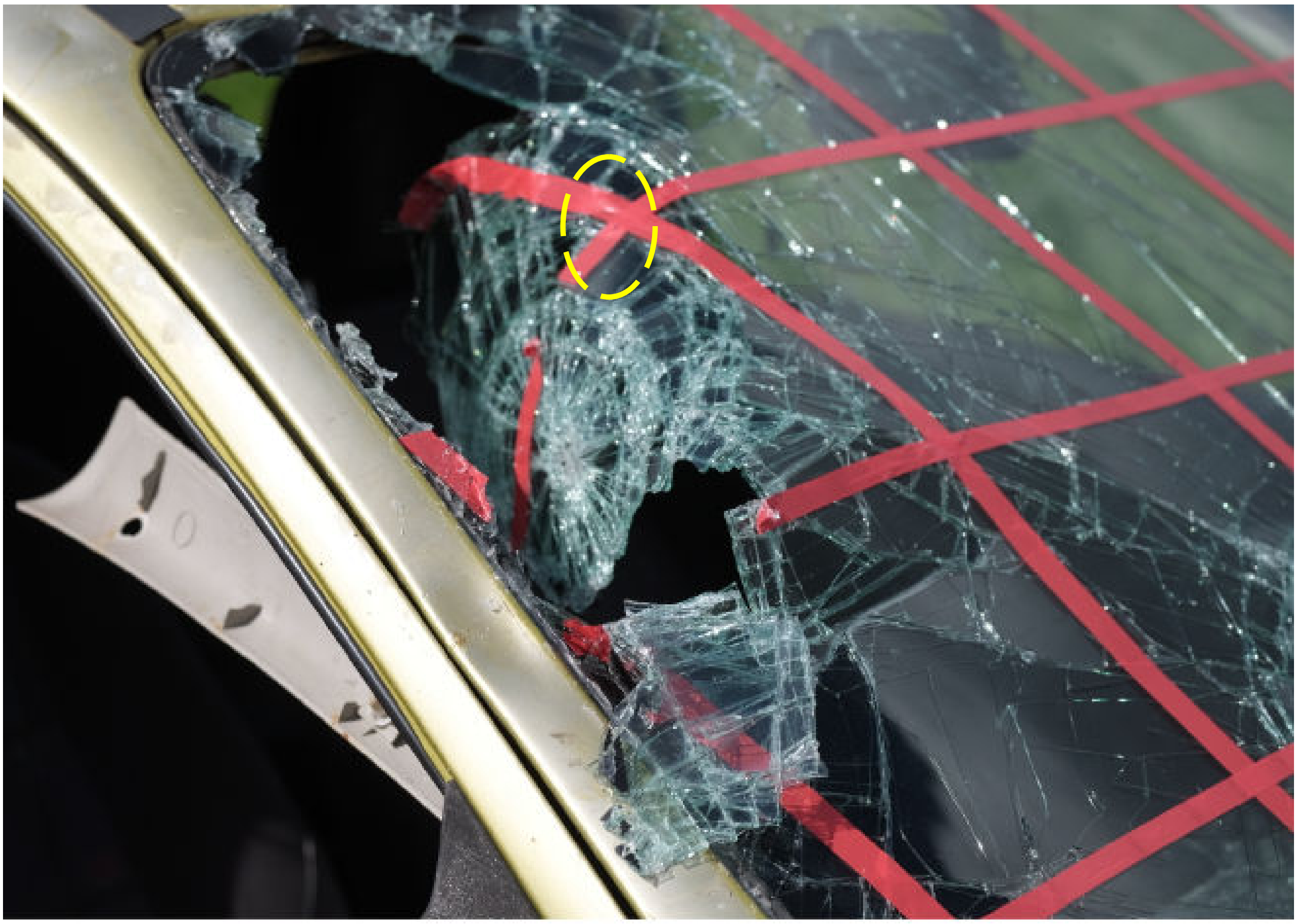

Figure 5. Spider-web type of deformation seen on the perforated area of the windscreen

3. METHOD FOR SIMULATING IMPACTS WITH WINDSCREEN PERFORATION

In order to properly analyze VRU impacts which result in windscreen perforations, simulations must be performed in a virtual environment.
Technically, for simulation software which rely on the multibody approach, such as PC Crash, vehicle deformations and their gradual evolution are virtually impossible to reproduce since the vehicle is considered a rigid body.

ISSN 2457 – 5275 (Online, English)
ISSN 1842 – 4074 (Print, Online, Romanian)

Although circular and spider-web deformations can be neglected and still obtain accurate kinematics since the integrity of the windshield is not severely affected, this is not the case for windshield perforations.
However, it is possible to simulate VRU intrusions in the passenger compartment or unbelted occupant ejections, if the exterior contour of the vehicle is altered.
The shape of any vehicle in PC Crash is defined by a tridimensional triangulated contour stored in a separate DirectX file for nearly all existing vehicle models.
The simulation method is comprised of an ensemble of procedures meant to modify the default design of the vehicle's frontal profile by inserting a cavity into the windshield in accordance with the configuration of the perforation.
The presented method was used to simulate the carried-out crash-test as it is shown further and it can be applied to any accident which results in windscreen perforations.
The first step consists in establishing the dimensional configuration of the perforation, which is done through the inspection and measurement of the windscreen's deformation.
An important parameter is the space of intrusion travelled by the dummy inside the passenger compartment, which can only be determined through video analysis.
In the case of real accidents, the injuries recorded by the human body can indicate the depth of the intrusion by evaluating how further tissue lacerations are relatively positioned to the head.
The second step consists in inserting the default contour of the vehicle and simulating the impact after applying the required adjustments.
The insertion of the cavity into the windscreen (see Figure 7) is realized by drawing a polyline onto the lateral profile of the vehicle in accordance to the depth of the penetration determined through video analysis, followed by applying the extrusion function of the program, as shown in Figure 6.

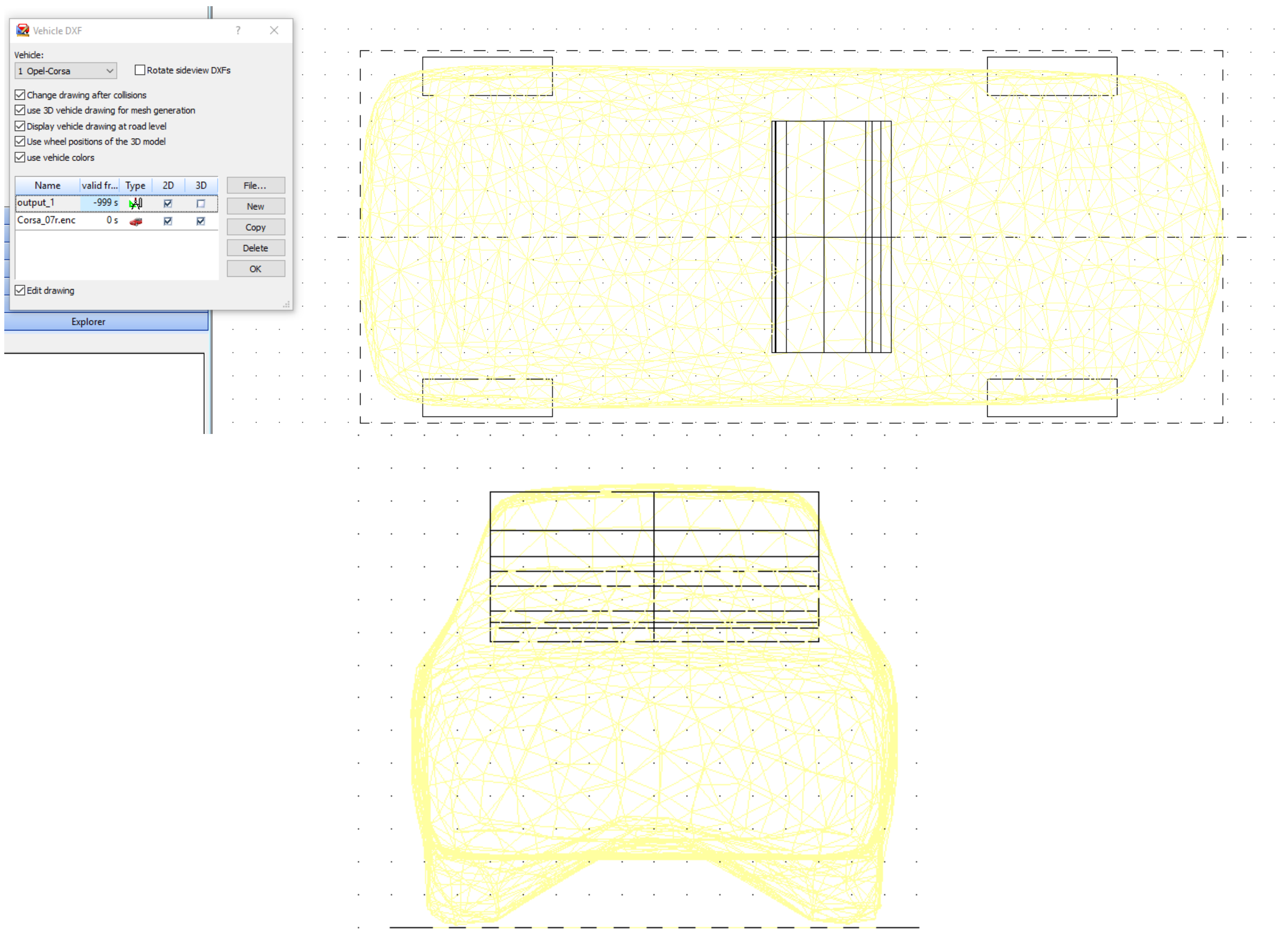

Figure 6. The extruded polyline marking the depth of the penetration

ISSN 2457 – 5275 (Online, English)
ISSN 1842 – 4074 (Print, Online, Romanian)

Figure 7. The cavity in the vehicle's windshield obtained by applying the extrusion function

The final step consists in simulating the impact after inserting the multibody model of the cyclist-dummy assembly and adjusting the cyclist posture, as well as the dimensions and masses of the assembly.
A significant amount of iterations are required to determine the defining kinematic and impact parameters.
Firstly, vehicle velocity and deceleration are iterated until conformance since these parameters are not particularly influenced by the impact due to the significant differences in mass and velocity between the vehicle and the dummy.
Secondly, the orientation of the bicycle at the time of impact must be established in order to further eliminate unknown variables.
The analysis of the deformations recorded by the vehicle and bicycle can indicate the angle of impact with reasonable accuracy.
Since the crash-test was also recorded via a drone and a high-speed camera, the angle of impact between the vehicle and the bicycle was determined with certainty.
Finally, the impact parameters, as well as friction coefficients must be iterated until the simulation resembles the kinematic behavior of the dummy as described by the video recordings.
The simulation was validated by obtaining a good congruence between the kinematic phases of the simulation and the carried-out crash-test, as it is presented in Figure 8.
In order to determine the influence of windscreen perforations over cyclist kinematics, the experimentally validated simulation was modified by inserting a default profile for the vehicle, thus rendering null the previous windscreen alterations.
By analyzing cyclist kinematics for both impacts with and without windscreen perforation, it has been determined that the duration of the cyclist transport phase is over five times higher for the case with windscreen perforation than for the case without, as shown in Table 1.
The cyclist throw distance was increased by 23% for the case with windscreen perforation compared to the case without, yet for higher vehicle impact velocities it is possible that the difference would result higher.
There is also a possibility for cases in which the resulting throw distance is diminished, with further research needed to clarify this aspect.

4. CONCLUSION

Windscreen perforations occur in particular cases of vehicle-VRU impacts generated at high vehicle impact velocities or due to windscreen delamination. Current state-of-art does not allow for windscreen stages of deformation to be simulated in multibody software. The simulation method presented in the paper allows a good kinematic sequence reconstruction of vehicle-VRU accidents with windscreen perforations by altering the exterior contour of the vehicle, as exemplified in the experimental case study.

ISSN 2457 – 5275 (Online, English)
ISSN 1842 – 4074 (Print, Online, Romanian)

The results of this study show that the generation of a windscreen perforation during an impact can increase the duration of the VRU's transport phase by over five times, which consequently increases the overall VRU throwing distance.

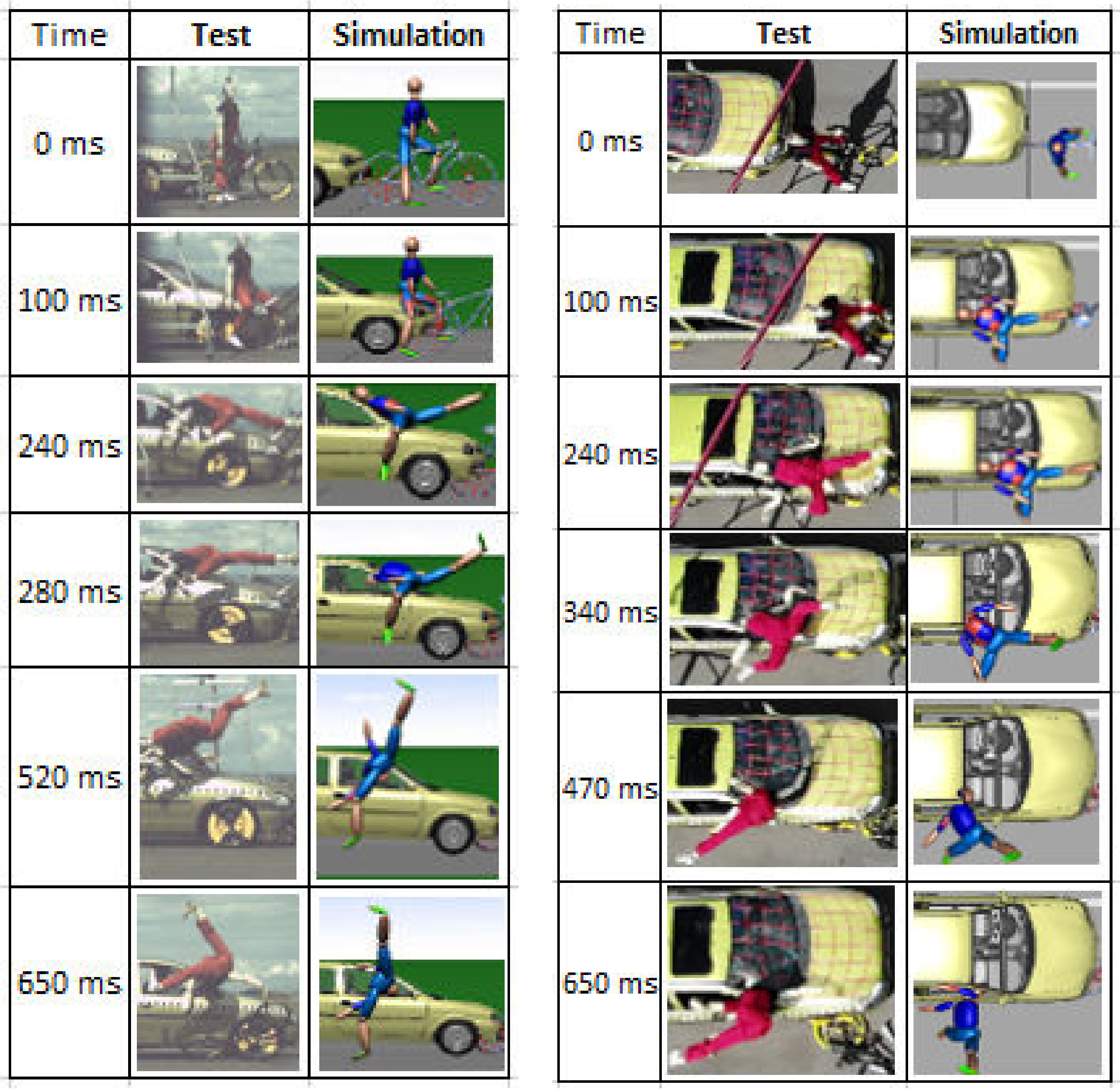

Figure 8. The kinematic phases of the carried-out crash-test and simulation

Table 1.
Cyclist transport phase duration for impacts with and without windscreen perforations

	With windscreen perforation	Without windscreen perforation
Head impact time (ms)	240	240
Launch moment (ms)	650	326
Transport phase duration (ms)	410	86

ISSN 2457 – 5275 (Online, English)
ISSN 1842 – 4074 (Print, Online, Romanian)

REFERENCES

1. Eppinger, H. Rolf, A biomechanical PEEEP show, Human Biomechanics and Injury Prevention. Springer. Tokyo. 2000.
2. Kimura, Chojiro. Experimental study on perforating eye injuries caused by the shattering of windshields, using a sled-dummy test device, The Keio Journal of Medicine, vol. 27(3-4), pag. 111-121, 1978.
3. Maki, Tetsuo; Kajzer, Janusz; Mizuno, Koji and Sekine, Yasufumi, Comparative analysis of vehicle–bicyclist and vehicle–pedestrian accidents in Japan, Accident Analysis & Prevention, vol. 35(6), pag. 927-940, 2003.
4. Müller-Jensen, Kei, and Walter Hollweck. Serious eye injuries produced by windshield damage-an actual problem in ophthalmology. SAE Technical Paper, No. 700912, 1970.
5. Otte, Dietmar. Design and structure of the windscreen as part of injury reduction for car occupants, pedestrians and bicyclists. SAE transactions 1994, pag. 1912-1922, 1994.
6. Pronk, Nicola; Fildes, Brian; Regan, Michael; Lenné, Michael; Truedsson, Niklas, & Olsson, Ted (2001). Windscreens and safety: a review. Vol. 183. Monash University Accident Research Centre Reports. 2001
7. Sances Anthony; Carlin, Fred; Kumaresan, Srirangam and Enz, Bruce, Biomedical engineering analysis of glass impact injuries. Critical Reviews, Biomedical Engineering, vol. 30(4-6), pag. 345-377, 2002.
8. Șoica, Adrian and Stelian Tarulescu, Impact phase in frontal vehicle-pedestrian collisions, International Journal of Automotive Technology, vol. 17(3), pag. 387-397, 2016.
9. Xu, Jun and Li, Yibing, Study of damage in windshield glazing subject to impact by a pedestrian's head. Proceedings of the Institution of Mechanical Engineers, Part D: Journal of Automobile Engineering, vol. 223(1), pag. 77-84, 2009.
10. Xu, Jun and Li, Yibing, Impact Behavior and Pedestrian Protection of Automotive Laminated Windshield. Manufacturing of Automotive Laminated Windshields. Vol. 21-37. Springer. Singapore. 2018.

RoJAE
Romanian
Journal of Automotive Engineering

AIMS AND SCOPE

The Romanian Journal of Automotive Engineering has as its main objective the publication and dissemination of original research in all fields of „Automotive Technology, Science and Engineering”. It fosters thus the exchange of ideas among researchers in different parts of the world and also among researchers who emphasize different aspects regarding the basis and applications of the field.

Standing as it does at the cross-roads of Physics, Chemistry, Mechanics, Engineering Design and Materials Sciences, automotive engineering is experiencing considerable growth as a result of recent technological advances. The Romanian Journal of Automotive Engineering, by providing an international medium of communication, is encouraging this growth and is encompassing all aspects of the field from thermal engineering, flow analysis, structural analysis, modal analysis, control, vehicular electronics, mechatronics, electro-mechanical engineering, optimum design methods, ITS, and recycling. Interest extends from the basic science to technology applications with analytical, experimental and numerical studies.

The emphasis is placed on contribution that appears to be of permanent interest to research workers and engineers in the field. If furthering knowledge in the area of principal concern of the Journal, papers of primary interest to the innovative disciplines of „Automotive Technology, Science and Engineering” may be published.
No length limitations for contributions are set, but only concisely written papers are published. Brief articles are considered on the basis of technical merit. Discussions of previously published papers are welcome.

Notes for contributors
Authors should submit an electronic file of their contribution to the ***Production office:*** www. siar.ro. All the papers will be reviewed and assessed by a series of independent referees.

RoJAE
Romanian
Journal of Automotive Engineering

ISSN 2457 – 5275 (Online, English)
ISSN 1842 – 4074 (Print, Online, Romanian)

The Scientific Journal of SIAR
A Short History

The engineering of vehicles represents the engine of the global development of the economy.
SIAR tracks the progress of the automotive engineering in Romania by: the development of automotive engineering, the development of technologies, and road transport services; supporting the work of the haulers, supporting the technical inspection and of the garage; encouraging young people to have a career in the automotive engineering and road haulage; stimulation and coordination of activities that promote an environment that is suitable for continuous education and improving of knowledge of the engineers; active exchange of ideas and experience, in particular for students, master students, PhD students, and young engineers, and dissemination of knowledge in the field of automotive engineering; cooperation with other technical and scientific organizations, employers' and socio-professional associations through organization of joint actions, of mutual interest.
By the accession to FISITA (International Federation of Automotive Engineering Societies) since its establishment, SIAR has been involved in achieving an overall professional community that is homogeneous in competence and performance, interactive, dynamic, and competitive at the same time, oriented towards a balanced and friendly relationship between people and the environment; this action will be constituted as a challenge worthy of effort and recognition.
The insurance of a favorable framework for the initiation and the development of cooperation of the specialists in this field of activity allows for an efficient and easy exchange of information, specific knowledge and experience; it supports the cooperation between universities and between research centers and industry; it speeds up the process of implementing the new technologies, it simplifies the identification of training and specialization needs of the personnel involved in the engineering of motor vehicles, transport, and road safety.
In order to succeed, ever since its founding, SIAR has considered that the stress should be put on the production and distribution, at national and international level, of a publication of scientific quality.

Under these circumstances, the development of the scientific magazine of SIAR had the following evolution:

1. RIA – Revista inginerilor de automobile (in English: ***Journal of Automotive Engineers***)
ISSN 1222 – 5142
Period of publication: 1990 – 2000
Frequency: Quarterly
Total number of issues: 30
Format: print, Romanian
Electronic publication on: www.ro-jae.ro
Type: Open Access
The above constitutes series nr. 1 of SIAR scientific magazine.

2. Ingineria automobilului (in English: ***Automotive Engineering***)
ISSN 1842 – 4074
Period of publication: as of 2006
Frequency: Quarterly
Total number of issues: 54
(including the March 2020 issue)
Format: print and online, Romanian
Electronic publication on: www.ingineria-automobilului.ro
Type: Open Access
The above constitutes series nr. 2 of SIAR scientific magazine (Romanian version).

3. Ingineria automobilului (in English: ***Automotive Engineering***)
ISSN 2284 – 5690
Period of publication: 2011 – 2014
Frequency: Quarterly
Total number of issues: 16
(including the December 2014 issue)
Format: online, English
Electronic publication on: www.ingineria-automobilului.ro
Type: Open Access
The above constitutes series nr. 3 of SIAR scientific magazine (English version).

4. *Romanian Journal of Automotive Engineering*
ISSN 2457 – 5275
Period of publication: from 2015
Frequency: Quarterly
Total number of issues: 21 (March 2020)
Format: online, English
Electronic publication on: www.ro-jae.ro
Type: Open Access
The above constitutes series nr. 4 of SIAR scientific magazine (English version).

Summary

Total of series:	*4*
Total years of publication:	*26 (11: 1990 – 2000; 15: 2006 – 2020)*
Publication frequency:	*Quarterly*
Total issues published:	*84 (Romanian), out of which, the last 37 were also published in English*